Surface Science 602 (2008) 2473–2477

Contents lists available at ScienceDirect

Surface Science

journal homepage: www.elsevier.com/locate/susc

Surface alloy model of $p(2 \times 2)$Sb/Cu(001) from LEED I/V data

Shougo Higashi [a], Hiroshi Tochihara [a], Valentin L. Shneerson [b], Dilano K. Saldin [b,*]

[a] Department of Molecular and Material Sciences, Kyushu University, Kasuga, Fukuoka 816-8580, Japan
[b] Department of Physics and Laboratory for Surface Studies, University of Wisconsin-Milwaukee, P.O. Box 413, Milwaukee, Wisconsin, WI 53201, USA

ARTICLE INFO

Article history:
Received 14 February 2008
Accepted for publication 16 May 2008
Available online 24 May 2008

Keywords:
Surface structure
Metallic surfaces
LEED
Chemisorption

ABSTRACT

We report on the re-determination of the structure of $p(2 \times 2)$Sb/Cu(001) from measured LEED I/V data. The structure solution is performed in two steps. First an approximate "image" of the surface structure model is found by an application to the measured data of the recently-proposed Phase and Amplitude Recovery and Diffraction Image Generation Method (PARADIGM). This reveals that the $p(2 \times 2)$ structure is formed by the protrusion of one atom out of four in the outermost surface layer. Since an Sb atom is larger than one of Cu, this suggests a possibility that the $p(2 \times 2)$ structure is formed by Sb substitution for one out of four Cu atoms in the outermost layer. Second, a tensor LEED refinement of the model suggested by the PARADIGM yields the same dominant top-layer substitutional model proposed in the earlier LEED study, but with a much lower reliability factor, making much less likely an admixture of other surface phases.

1. Introduction

The determination of spatial arrangements of atoms on a surface is important not only for fundamental science, but also for industrial applications in areas as diverse as heterogeneous catalysis and microelectronics. Databases of surface structures [1] suggest that low energy electron diffraction (LEED) [2] is a dominant technique for acquiring such information. From the point of view of surface structure determination, the strong interaction of low energy electrons with a material has the beneficial effect of largely limiting the scattering of the electrons to a handful of the outermost atomic layers. Yet, the very strength of this interaction also makes the interpretation of LEED data very difficult, due to strong multiple scattering. The traditional method of surface structure determination by LEED is the trial-and-error fitting of measured intensity versus energy distributions with simulations of such distributions from guessed surface structural models. Once the general features of a structural model have been successfully guessed, a refinement of this model may be performed by a systematic variation of a limited number of structural parameters in order to optimize those parameters. Due to an exponential scaling of the number of structural variations with the number of such parameters, this is a hard optimization problem [3] of the so-called NP (non-polynomial) complete class. A correct guess of an approximate structure enables the number of unknown parameters to be kept low enough to make such a method tractable. Such a method has been successfully used to determine coadsorbed structures as complicated as Al(111)-(2×2)-Na,K(Rb,Cs) [4], Ag(001)-(3×3)-Na,K [5], Cu(001)-$(2\sqrt{2} \times \sqrt{2})R45°$-Mg,Li [6,7], Cu(001)-$(\sqrt{5} \times \sqrt{5})R26.7°$-Mg,K(Cs) [8], Cu(001)-$c(2 \times 2)R45°$-Mg,Bi [9], Cu(001)-$c(6 \times 4)$-Mg,Bi [8], Cu(001)-$\left(\sqrt{5} \times \sqrt{5}\right)R26.7°$-Bi,K(Cs) [10], Cu(001)-$(4 \times 4)$-Mg,Bi(Sb) [11], and Cu(001)-$c(6 \times 4)$-Mn,Bi [12]. The number of structural models to be tested was limited by classifying the direct and indirect interactions of dissimilar atoms on a surface [13]. However, even with such educated guesses, the number of models which need to be refined may be very large. For example, for the Cu(001)-$c(6 \times 4)$ structure formed by coadsorption of the Mn and Bi denoted above as Cu(001)-$c(6 \times 4)$-Mn,Bi [12], even exploiting the information of the coverage and surface symmetry, at least 30 models needed to be considered as starting points for a systematic refinement scheme. Of course, even then, there was no guarantee that the correct model was amongst those chosen as starting points for refinement. The ultimate bottleneck to the general application of such a method for the determination of a surface structure whose characteristics are completely unknown is the correctness of the initial guess of the structural model, a process for which there is as yet no systematic prescription.

Other techniques, such as protein X-ray crystallography, are able to determine much more complicated structures by following a two-pronged strategy: initially, an objective algorithm applied directly to the measured data to suggest a likely atomic model; a subsequent refinement of this approximate model from systematic small variations of structural parameters determines the atomic model which best agrees with the data.

It is in order to fill the need for this initial step for surface crystallography by LEED, that Saldin and co-workers [14–17] have

* Corresponding author. Tel.: +1 414 229 6423; fax: +1 414 229 5589.
E-mail address: dksaldin@uwm.edu (D.K. Saldin).

0039-6028/$ - see front matter © 2008 Elsevier B.V. All rights reserved.
doi:10.1016/j.susc.2008.05.022

developed a direct method for LEED which suggests such a starting point by an objective algorithm applied to measured LEED data. This is a generalization to the LEED multiple scattering problem of a method previously developed for surface X-ray diffraction (SXRD) [18–23]. The method exploits two main features, (1) the fact that the experimental data may be regarded as a sum of two sets of scattering paths: (a) those which involve scattering from just the known bulk structure and (b) those which include scattering by the unknown surface atoms whose positions deviate from those expected from the bulk structure; and (2) the breaking of the periodicity normal to the surface which circumvents the Bragg condition, and hence allows an oversampling [24] of the scattered amplitudes in this direction. An iterative algorithm which alternately satisfies constraints in real and reciprocal space reconstructs a distribution of likely atom positions in a 3D surface unit cell. This provides an immediate visualization of a starting model for refinement by conventional methods, and has been termed the Phase and Amplitude Recovery and Diffraction Image Generation Method (PARADIGM for short) [17,23].

Before the application of a new method of analysis to experimental data from an unknown structure, of course its validity needs to be established by tests on data which have previously been analyzed by established methods. Our new algorithm has previously been applied to (1) the recovery of the structure of $c(2\times2)$Br/Pt(110) [14], where the algorithm correctly found the short-bridge adsorption sites of the Br adatoms on a Pt(110) surface previously suggested by scanning tunneling microscopy (STM), density functional theory (DFT), and a conventional LEED [25]; (2) the recovery of the (3×1)Br/Pt(110) structure [15], in agreement with conventional LEED analysis and DFT [26]. In this structure, the Br atoms reside on every third short-bridge and long-bridge sites, and it was shown that the method was capable of recovering the location of adatoms on inequivalent sites in the surface unit cell; and (3) the recovery of the quasi-hexagonal structure of (5×1)Ir(100) [27], as well as the structure of (5×1)H/Ir(100), where adsorption of H causes one of the 6 strained atomic rows in the clean surface to "pop out" of the top-layer to form a single-atom-wide "nanowire" [28], and the structures of 0.4 ML and 0.8 ML (5×1)Fe/H/Ir(100) where Fe atoms decorate the Ir nanowire to various extents [29–30].

In the following we describe another test, this time on the system $p(2\times2)$-Sb/Cu(100) initially studied by Al Shamaileh et al. [31]. Those authors suggested that despite a large size mismatch between Sb (atomic radius 1.450 Å) and Cu (atomic radius 1.278 Å) a surface alloy is formed at room temperature in which Sb atoms substitute Cu atoms in the outermost layer. However, due to the relatively high Pendry R-factor [32] ($R_p = 0.26$) they found for this model, they did not rule out the possible coexistence of other surface phases, such as (2×2), (1×1), and $c(2\times2)$ phases.

2. Paradigm for LEED

The details of the theory of the PARADIGM are given in our earlier publications [14,15,17,23]. A summary is presented here. The experimental data consist of a set of measured intensities $\{I_\varepsilon\}$, where $\varepsilon \equiv (\mathbf{g}, E)$ represents a folded index specifying the Bragg reflection $\mathbf{g}$ and electron energy, E. Apart from a scaling factor, one may write

$$I_\varepsilon = |F_\varepsilon|^2$$

the square modulus of a structure factor F_ε of the surface. The latter may be regarded as a sum

$$F_\varepsilon = B_\varepsilon + S_\varepsilon$$

of scattered amplitudes from two classes of scattering paths. The amplitude B_ε arises from the sum of all possible multiple scattering paths of the incident electron with the (known) bulk structure,

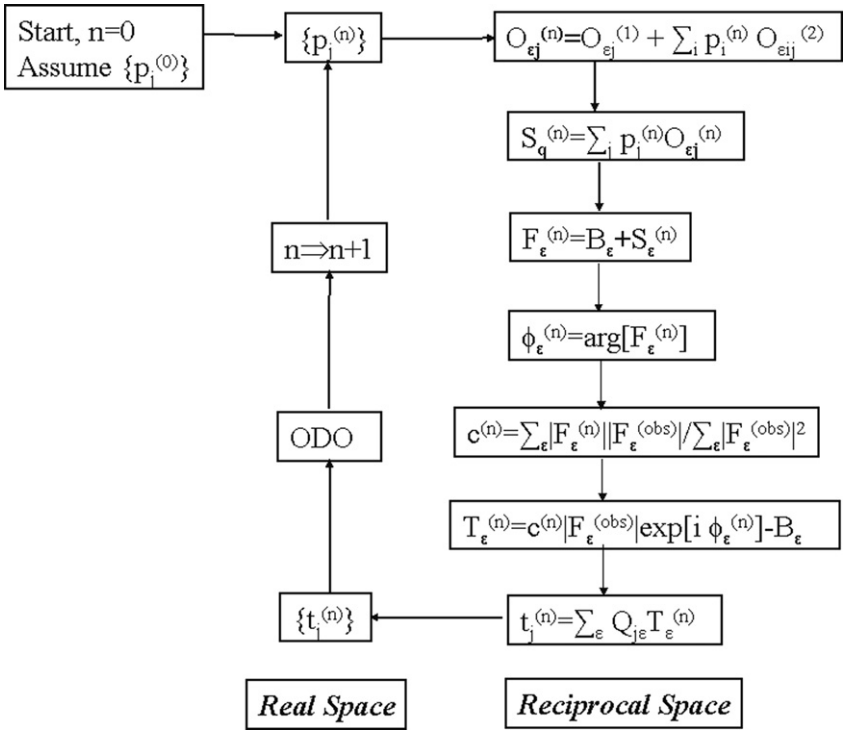

Fig. 1. Flow chart of the LEED PARADIGM program. The operations on the left-hand side of the flow chart are performed on the current estimate of the atom distribution in real space; The symbols ODO represent object domain operations, in this case an atomicity constraint (see text for details) that transforms an output real-space atom distribution $\{t_j\}$ at a particular iteration to an input distribution $\{p_j\}$ for the next application of constraints to measured experimental data. Operations on the right-hand side of the flow chart constrain the diffracted amplitudes to square roots of the measured intensities. Symbols as defined in the text and in Ref. [16]. The matrix elements $Q_{j\varepsilon}$ are defined by the orthogonality relation $Q_{j\varepsilon}O_{\varepsilon i} = \delta_{ji}$. The matrix $\mathbf{Q}$ is calculated by singular value decomposition of the matrix $\mathbf{O}(\equiv\{O_{\varepsilon j}\})$.

which may be calculated exactly once from multiple scattering theory, since this part of the structure is known. The amplitude S_ε includes scattering from the (unknown) surface structure to be determined. Of course, due to multiple scattering between surface and bulk, these amplitudes have to include scattering by atoms in the bulk. Since $|F_\varepsilon|^2$ is measurable and B_ε is known, the recovery of the unknown amplitudes S_ε from the two former sets of quantities may be likened to holographic reconstruction, where the measured diffracted intensities $\{|F_\varepsilon|^2\}$ may be regarded as constituting a hologram, $\{B_\varepsilon\}$ elements of a reference wave, and $\{S_\varepsilon\}$ those of an object wave [33]. A key to determining the unknown surface structure is to write

$$S_\varepsilon = \sum_j p_j O_{\varepsilon j},$$

where $\{p_j\}$ is the unknown distribution of surface atoms (to be determined) on a suitably-chosen grid over the surface unit cell, and $O_{\varepsilon j}$ is a so-called *elementary object wave* [34] which may be calculated for each grid point j and each value of ε, on the basis of a *quasidynamical approximation* [35]. As has been pointed out [17] the elementary object wave itself depends on the very distribution $\{p_j\}$ sought *via*:

$$O_{\varepsilon j} = O^{(1)}_{\varepsilon j} + \sum_i p_i O^{(2)}_{\varepsilon ij}.$$

due to the fact that it is necessary to take account of at least two scatterings of an incident LEED electron from a surface, once on its inward path, and once on its outward one.

For an assumed surface atomic species, the two constituent parts, $O^{(1)}_{\varepsilon j}$ and $O^{(2)}_{\varepsilon ij}$, of the elementary object waves may be calculated on the surface unit cell grid from a standard LEED program [36], for a given bulk structure, independent of a knowledge of the actual surface structure to be determined, as described in our earlier publications [14–17]. A flow chart of the algorithm for determining the unknown distribution $\{p_j\}$ of surface atoms is shown in Fig. 1.

The object domain operations, represented by the symbols ODO on the flow chart are an atomicity constraint, used to modify the output distribution $\{t_j\}$ at any particular iteration to an input distribution $\{p_j\}$ at the next iteration. In the present work, these operations consist of first finding the greatest value of t_j and then setting to zero all voxel values within an assumed atomic radius of it. The next highest value of t_j is the found and all voxels within an assumed atomic radius of it set to zero, and the process repeated until the search for the voxel results in a next highest value is zero. The resulting distribution is taken to be $\{p_j\}$ for the next iteration.

3. Experimental details

We have obtained new experimental LEED data from the $p(2 \times 2)$-Sb/Cu(100) surface previously studied by Al Shamaileh et al. [31], using an ultra-high vacuum (UHV) chamber equipped with a commercial LEED apparatus under a base pressure of 10^{-10} torr. A clean Cu(001) surface was prepared by cycles of Ar+ sputtering (1.5 KV, 1.5 uA) followed by the sample annealing at 900 K for about 20 min. This procedure was repeated until sharp and brilliant integer-order spots of the Cu substrate were obtained. Then Sb was evaporated onto the Cu surface from a home-made Knudsen cell at room temperature. Extra $p(2 \times 2)$ Bragg spots were observed at sample temperature of 130 K. The intensities of 4 inequivalent integer-order Bragg reflections, (10), (11), (20), and (12), and 3 half-integer-order reflections (1/2 0), (3/2, 1/2), (1/2, 1/2) were recorded by a computer-controlled CCD camera in an energy range of 50–420 eV for normal incidence of the LEED electrons. The total energy range (i.e. the sum of the energy ranges of all the LEED beams) was 1449 eV. Details of the experiments were similar to those of the previous studies [5–13].

4. Results

Calculated atomic phase shifts of Cu are used as an input to the PARADIGM. Fig. 2 shows the distribution $\{p_j\}$ of atoms in a $p(2 \times 2)$ unit cell of the outermost surface layer found after 62 cycles around the flow chart of Fig. 1. The final distribution $\{p_j\}$ contains non-zero values at just 4 voxels. Of these four voxels, one (Fig. 2) is located at a height of about 0.5 Å above the other three, confirming the top-layer substitutional surface alloy model suggested previously on the basis of a conventional LEED analysis [31].

We then performed a structural refinement of the above surface alloy model by means of A Barbieri/Van Hove symmetrized automated tensor LEED (SATLEED for short) package [37]. The dashed line in Fig. 3 shows the surface unit cell corresponding to the image recovered by the PARADIGM. In the SATLEED analysis, ten phase shifts ($l_{max} = 9$) were used to calculate atomic scattering. The programs searched for agreement with the experiment by minimizing RP [32].

The real part of the inner potential was determined during the course of the theory-experiment fit. To represent the inelastic scattering, damping was represented by an imaginary part of the potential, V_{oi}, of −5.0 eV. The error range of structural parameters was obtained from the variance of the R_P factor, $\Delta R = R_{min}\sqrt{8V_{oi}/\Delta E}$ [32] where R_{min} is the minimum R_P factor achieved, and ΔE is the total energy range.

An excellent minimum R_p value of 0.16 was achieved in the course of the structural optimization. The best fit I/V curves are compared with the corresponding experimental results in Fig. 4. The visual quality of the fit is also seen to be excellent. The optimized structural parameters with error bars are shown in Table 1.

5. Discussion

As pointed out earlier, the previous LEED study of the same system by Al Shamaileh et al. [31] pointed to essentially the same surface alloy model, but the R_P value quantifying the agreement between the best-fit model and experiment was significantly higher ($R_P = 0.26$). Al Shamaileh et al. attributed their relatively high R-factor to the potential coexistence of other surface phases, such as (2×2), (1×1), and $c(2 \times 2)$ as mentioned above [31]. However, given the much lower R_p value found in our work, application of

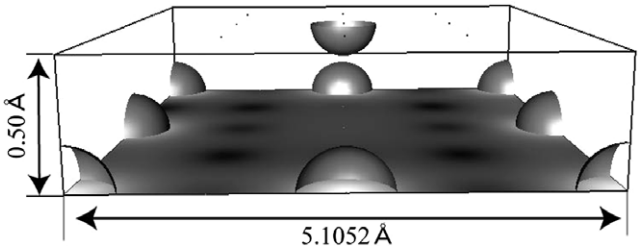

Fig. 2. 3D probability distribution of atoms in a $p(2 \times 2)$ surface unit cell, as recovered by the LEED PARADIGM algorithm [16]. An intensity map of the distribution at the bottom of the 3D surface unit cell before final application of the atomicity constraint is shown as a continuous distribution. Light regions of the map on this plane indicate regions of high values of the atom probability distribution, while dark regions represent the lowest values. Repeated applications of the atomicity constraint (see text) ultimately leads to distribution which has zero values at all but 5 voxels in the $p(2 \times 2)$ surface slab shown. These non-zero voxels are indicated by the spheres (or parts thereof if they are at the boundaries of the $p(2 \times 2)$ surface unit cell), whose radii are proportional to the values of the atom distribution $\{p_j\}$ at those voxels.

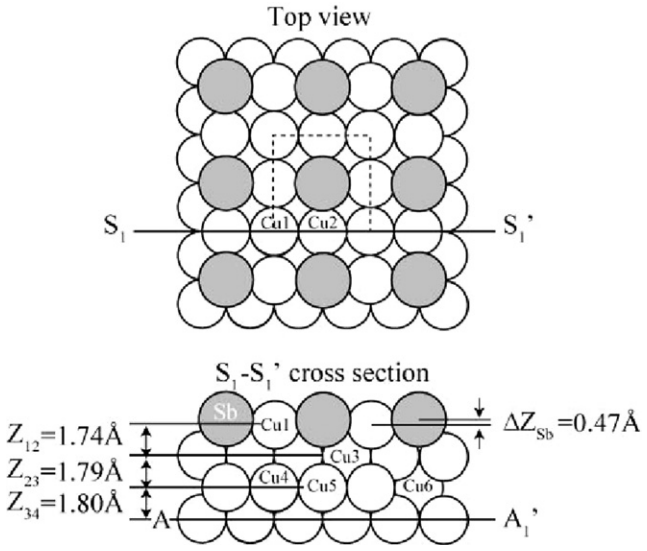

Fig 3. Top and cross sectional views of the structure of $p(2 \times 2)$-Sb/Cu(001). Gray circles represent Sb atoms and white circles represent the Cu atoms. Inequivalent Cu atoms are labeled by different numbers.

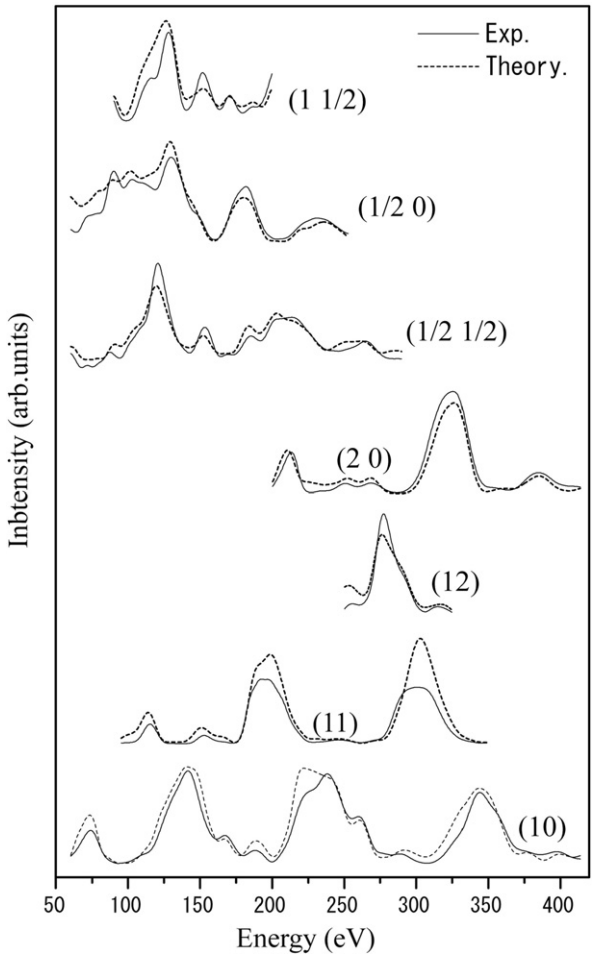

Fig. 4. Comparison of experimental and theoretical I/V curves of 7 inequivalent Bragg spots.

Occam's razor suggests it more reasonable to postulate a single $p(2 \times 2)$ surface alloy phase, without complicated admixtures with other phases.

Table 1
Optimum parameters of the best-fit structure of $p(2 \times 2)$-Sb/Cu(001) shown in Fig. 3

Atom	Lateral displacement (Å)		Height (Å)
	x-axis	*y*-axis	
Sb1			5.88 ± 0.04
Cu1			5.37 ± 0.02
Cu2			5.42 ± 0.03
Cu3	0.01 ± 0.13	0.01 ± 0.13	3.63 ± 0.02
Cu4			1.84 ± 0.02
Cu5			1.80 ± 0.02
Cu6			1.79 ± 0.01

Lateral displacements are measured from the hollow-site position in the second Cu layer.

Assuming the existence of such a single surface phase, there are at the very least 4 possible structural adsorption sites for an Sb atom in $p(2 \times 2)$Sb/Cu(001), namely, a hollow site, a bridge site, an on-top site and a substitution site, such as depicted in Fig. 1 of Ref. [31]. With a conventional trial-and-error method, one would need to calculate the I–V curves for at least each of these four models to find the correct structure. Indeed this is precisely what was done in the previous LEED study [31] to eliminate the other Sb atom sites. Although this is a relatively trivial example, we have shown that an application of the LEED–PARADIGM algorithm to experimental LEED data leads directly to the correct substitutional surface alloy model. Although precise structural parameters still need to be deduced from a conventional LEED refinement procedure, starting from the correct model leads to a saving of about a factor of 4 of computer time in this case.

As for possible reasons for the much lower value of R_P (0.16) we found for the optimal structure compared with the value (0.26) found by Al Shamaileh et al. [31], we point out that: (i) we measured the I–V curves of $p(2 \times 2)$-Sb on the surface when the intensity of the (1/2, 1/2) spots exhibited the maximum intensity versus deposition time. This is designed to maximize the signal from the ordered superstructure; (ii) we measured the I–V curves at a sample temperature of 130 K in order to minimize non-structural thermal vibration effects, in contrast to Al Shamaileh et al. [31] who performed the measurements at room temperature. Consequently, our measured I–V curves show more prominent peaks and shoulders as may be seen by comparing our Fig. 4 with Fig. 2 of Ref. [31].

6. Conclusions

In summary, we have presented the results of a reinvestigation of the $p(2 \times 2)$Sb/Cu(001) structure formed by the room temperature deposition of Sb on this surface, using a new direct method, PARADIGM, for LEED [17]. When applied to our experimental data, the method rapidly reveals a corrugated outermost surface layer, with one out of 4 atoms at a greater height above the substrate. This immediately suggests a substituted Sb model, consistent with a previous study [31]. Based on this starting model and a conventional refinement of high-quality measured I–V curves, it was reconfirmed that a model involving the substitution of Sb atoms for one in every four Cu atoms on a Cu(001) surface is the structure of $p(2 \times 2)$ Sb/Cu(001). A subsequent refinement by a conventional tensor LEED analysis led to a Pendry R-factor (R_p) as low as 0.16, probably excluding the earlier suggestion [31] of the possible coexistence of other surface phases.

This relatively simple structure allowed us a further test the recently-proposed PARADIGM algorithm for rapidly finding a likely surface model directly from experimental data, as a starting point for subsequent refinement by conventional LEED methods. Although, in this case, the savings of computer time are relatively modest (a factor of about 4), the success of the scheme is an

encouraging sign of its potential for much more significant time savings for more complicated structures with a much larger number of potential structural models.

Acknowledgements

SH gratefully acknowledges support for this work from Research Fellowships of the Japan Society for the Promotion of Science for Young Scientists. DKS acknowledges financial support from the US Department of Energy (Grant Number DE-FG02-84ER45076).

References

[1] P.R. Watson, M.A. Van Hove, K. Hermann, NIST Surface Structure Database, Version 4.0 (NIST Standard Reference Database 42, 2002).
[2] M.A. Van Hove, W.H. Weinberg, C.-M. Chan, Low Energy Electron Diffraction, Springer, Berlin, 1986.
[3] J.B. Pendry, K. Heinz, W. Oed, Phys. Rev. Lett. 61 (1988) 2953.
[4] S.V. Christensen et al., Phys. Rev. Lett. 76 (1996) 1892.
[5] S. Mizuno, M. Imaki, H. Tochihara, Surf. Rev. Lett. 8 (2001) 653.
[6] M.S. Chen, S. Mizuno, H. Tochihara, Surf. Sci. 486 (2001) L480.
[7] M.S. Chen, S. Mizuno, H. Tochihara, Surf. Sci. 514 (2002) 94.
[8] T. Shirasawa, M.S. Chen, S. Mizuno, H. Tochihara, Surf. Sci. 530 (2003) L307.
[9] T. Shirasawa, S. Mizuno, H. Tochihara, Surf. Sci. 538 (2003) L488.
[10] M.S. Chen, S. Mizuno, H. Tochihara, Surf. Sci. 536 (2003) L415.
[11] S. Higashi, T. Shirasawa, S. Mizuno, H. Tochihara, Surf. Sci. 588 (2005) 167.
[12] S. Higashi, T. Ohshima, S. Mizuno, H. Tochihara, Surf. Sci. 600 (2006) 591.
[13] H. Tochihara et al., Vacuum 74 (2004) 121.
[14] D.K. Saldin, A. Seubert, K. Heinz, Phys. Rev. Lett. 88 (2002) 115507.
[15] A. Seubert, K. Heinz, D.K. Saldin, Phys. Rev. B 67 (2003) 25417.
[16] R.J. Harder, D.K. Saldin, in: W. Schattke, M.A. Van Hove (Eds.), Solid State Photoemission and Related Phenomena, Wiley-VCH, Weinheim, 2003, p. 370.
[17] D.K. Saldin, V.L. Shneerson, Special Issue of J. Phys.: Condens. Matter Commemorating the 65th Birthday of Prof. Sir John Pendry, in press.
[18] D.K. Saldin, R.J. Harder, V.L. Shneerson, W. Moritz, J. Phys.: Condens. Matter 13 (2001) 10689.
[19] D.K. Saldin, R.J. Harder, V.L. Shneerson, W. Moritz, J. Phys.: Condens. Matter 14 (2002) 4087.
[20] D.K. Saldin, V.L. Shneerson, R. Fung, Physica B 336 (2003) 16.
[21] P.F. Lyman, V.L. Shneerson, R. Fung, R.J. Harder, E.D. Lu, S.S. Parihar, D.K. Saldin, Phys. Rev. B 71 (2005) 115434.
[22] P.F. Lyman, V.L. Shneerson, R. Fung, S.S. Parihar, H.T. Johnson-Steigelman, E.D. Lu, D.K. Saldin, Surf. Sci. 600 (2006) 424.
[23] R. Fung, V.L. Shneerson, P.F. Lyman, S.S. Parihar, H.T. Johnson-Steigelman, D.K. Saldin, Acta Cryst. A63 (2007) 239.
[24] J. Miao, P. Charalambous, J. Kirz, D. Sayre, Nature 400 (1999) 342.
[25] V. Blum, L. Hammer, K. Heinz, C. Franchini, J. Redinger, K. Swamy, C. Deisl, E. Bertel, Phys. Rev. B 65 (2002) 165408.
[26] C. Diesl, K. Swamy, N. Memmel, E. Bertel, C. Franchini, G. Schneider, J. Redinger, S. Walter, L. Hammer, K. Heinz, Phys. Rev. B 69 (2004) 195405.
[27] A. Ignatiev, A.V. Jones, T.N. Rhodin, Surf. Sci. 30 (1972) 573.
[28] L. Hammer, W. Meier, A. Klein, P. Landfried, A. Schmidt, K. Heinz, Phys. Rev. Lett. 91 (2003) 156101.
[29] A. Klein, A. Schmidt, L. Hammer, K. Heinz, Europhys. Lett. 65 (2004) 830.
[30] K. Heinz, L. Hammer, A. Klein, A. Schmidt, Appl. Surf. Sci. 237 (2004) 519.
[31] E. Al Shamaileh, K. Pussi, T. McEvoy, M. Lindroos, G. Hughes, K.A. Cafolla, Surf. Sci. 566 (2004) 52.
[32] J.B. Pendry, J. Phys. C 13 (1980) 937.
[33] D.K. Saldin, P.L. De Andres, Phys. Rev. Lett. 64 (1990) 1270.
[34] A. Szöke, Phys. Rev. B 47 (1993) 14044.
[35] N. Bickel, K. Heinz, Surf. Sci. 163 (1985) 435.
[36] M.A. Van Hove, S.Y. Tong, Surface Crystallography by LEED, Springer, Berlin, 1979.
[37] M.A. Van Hove, W. Moritz, H. Over, P.J. Rous, A. Wander, A. Barbieri, N. Materer, U. Starke, G.A. Somorjai, Surf. Sci. Rep. 19 (1993) 191.